

A kinetic study of CO₂ sorption improvement in the CA-CNTs mixed matrix membrane

E T S Wong¹, Z A Jawad¹ *, B L F Chin¹, S K Wee²

¹ Department of Chemical Engineering, Faculty of Engineering and Science, Curtin University Malaysia, CDT 250, 98009 Miri, Sarawak, Malaysia

² Department of Petroleum Engineering, Faculty of Engineering and Science, Curtin University Malaysia, CDT 250, 98009 Miri, Sarawak, Malaysia

Abstract. Greenhouse emission notably carbon dioxide (CO₂) in the atmosphere have been increasing significantly over the last century. Hence, there is a need to address this issue to minimize the adverse environmental effects. Membrane separation is one solution that could potentially help in this endeavour. Among the many types of membranes available, mixed matrix membrane (MMM) is the most promising with the potential to surpass the many deficiencies present in both inorganic and polymeric membranes. In this study, results confirmed that incorporation of functionalized CNTs increases CO₂ permeance. Hence, the different loadings of MWCNTs-F were investigated to find the optimum gas separation performance. From this optimization study, excellent MMM performances in terms of CO₂ permeance were shown in 0.1wt% loading of MWCNTs-F. This superior performance was attributed to a good homogeneous dispersion of MWCNTs-F in the CA matrix which consequently enlarged the free volumes between the polymer chains and improved the polymer nano particulate interface. Apart from this, a kinetic sorption study showed improvements in the CO₂ solubility coefficient over previous related work at $14.9601 \times 10^{13} \text{ cm}^3(\text{STP})/\text{cm}^4 \cdot \text{cmHg}$. Hence, the usage of lower acetyl content is proven to be capable of increasing the CO₂ solubility coefficient.

1. Introduction

Over the years, greenhouse gasses (GHGs) such as carbon dioxide (CO₂) have been increasing significantly in the earth's atmosphere [1]. This has serious implications to the Earth from global warming to weather changes [2]. CO₂ gas is the main subject matter among these GHGs as it is released in large quantities compared to rest [2]. Hence, a few incentives have been taken to reduce the release of CO₂ into the environment [3].

The usage of membranes in separation is one that could possibly help in this endeavour as it addresses the many issues plaguing commercial CO₂ capture [4]. Some of the polymeric materials available are cellulose acetate (CA), polyimide (PI), polysulfone (PSF), polyethersulfone (PES), and polycarbonates (PC). Commercially, only PI and CA have been mainly used for CO₂/CH₄ and CO₂/N₂ separations [5]. This is due to the excellent gas separation performance of these 2 polymers [6]. Mixed matrix membrane (MMM) which is made up of a polymer matrix and an inorganic filler is currently the most promising way forward. [7]. Carbon nanotubes (CNTs) were proved to be able to transport light gases many times faster than any other known microporous material [8]. However, the poor distribution and weak interfacial interaction of the inorganic fillers within the polymer matrix leads to the formation of unselective channels within the membranes [9]. Thus, there is need to enhance the compatibility between the inorganic fillers and the polymer matrix within the MMMs.



The main objective of this research study is to synthesise MMM from cellulose acetate (CA) polymer matrix of 39% acetyl group and CNTs with high CO₂ permeance and solubility coefficients for the first time. From previous works, CA polymer containing a high acetyl content was documented to have high CO₂ permeance and sorption coefficients. However, it is known to easily plasticize upon exposure to high CO₂ pressures. Hence, in this study CA membranes with a lower acetyl group (39%) would be fabricated and compared in terms of CO₂ permeance and sorption coefficients. Results reveals that a lower acetyl group (39%) improves the membrane's CO₂ permeance and sorption coefficients.

2. Experimental

2.1 Fabrication of Cellulose Acetate Membrane (CA-M)

The cellulose acetate membrane (CA-M, Table 1) was prepared based on the method published in previous work [10].

2.2 Fabrication of Mixed Matrix Membrane (CA-CNTs)

Pristine MWCNTs (MWCNTs-P) was functionalized using β -CD employing Chen's soft cutting method [11]. A set quantity of MWCNTs-P or Functionalized MWCNTs (MWCNTs-F) was added to the CH₃ COOH and H₂O before it is sonicated, as shown in Table 1. Stirring of the suspension was then instigated for 4 hr for better particle distribution of the MWCNTs. After that, CA was added gradually into the suspension of 55°C and stirred for 3 hr till it is dissolved completely followed by the synthesis method described in previous published work [10].

Table 1. The composition of the membranes fabricated.

Sample Description	Polymer	Solvent mixture (ratio 70:30)			MWCNTs		
		CA (wt%)	CH ₃ COOH (wt%)	H ₂ O (wt%)	Total Filler ^a (wt%)	Solid base MWCNTs ^b (wt%)	Solid base β -CD ^c (wt%)
CA-M	15	63	27	0.000	0.000	0.000	
MMM-0.05P	15	62.993	26.997	0.050	0.005	0.000	
MMM-0.1F	15	63.780	26.910	0.100	0.010	0.300	
MMM-0.2F	15	62.544	26.805	0.200	0.021	0.630	
MMM-0.05F	15	62.890	26.953	0.050	0.005	0.152	

^aTotal filler = embedded MWCNTs into CA polymer. ^bSolid base MWCNTs = total filler x CA / (1 - total base filler (1 + 30)). ^cSolid base β -CD = 30 x solid base MWCNTs

2.3 Kinetic Sorption Study

Membrane sorption experiments were carried out using a previous published procedure [12].

3. Results and Discussions

3.1 Integration of MWCNTs into CA Polymer.

3.1.1 Membrane Characterization. Scanning Electron Microscope (SEM) used to observe the physical structure and morphology of the cellulose acetate (CA) membrane, MMM-0.05P and the MMM-0.05F. Based on Figure 1a-b, it can be seen that the CA membrane has a smooth surface with a compact polymer layer near to the membrane/air interface. However, when pristine Multi-Walled Carbon Nanotubes (MWCNTs-P) were embedded into the CA in Figure 1c-d, it was found to have almost a nonexistent compact layer as compared to the neat CA membrane.

This was due to the MWCNTs-P being agglomerated within the polymer matrix from the strong van der Waals forces and their hydrophobic nature [13]. This inferred that the MWCNTs-P had a stronger interaction between each other in contrast to the polymer matrix [14]. This phenomenon was schematically described by Ahmad et al. [10].

Conversely, Figure 1e-f demonstrates a thinner compact layer at the membrane/air interface as compared to the pure CA membrane. No agglomeration was present in the polymer matrix indicating a better interaction between the CNTs with the CA. The beta cyclodextrin (β -CD) used to functionalize the MWCNTs (MWCNTs-F) helped eliminate agglomeration by shortening the MWCNTs and removing the van der Waals forces between them [15].

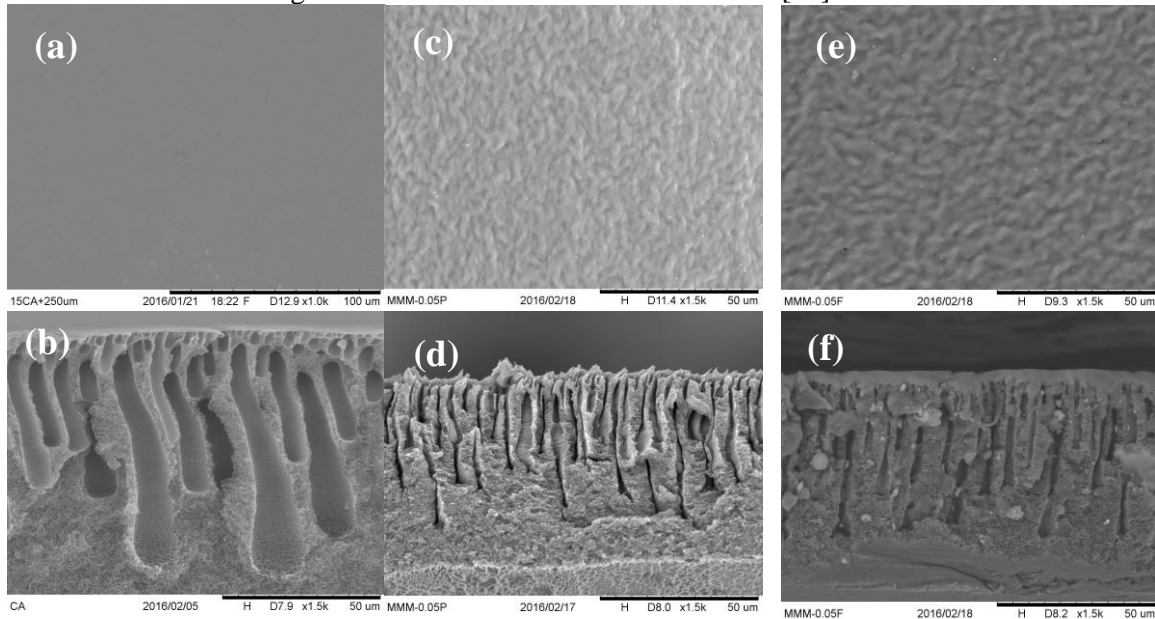


Figure 1. SEM morphologies of surface and cross section of (a-b) CA membrane and mixed matrix membrane with (c-d) MWCNTs-P (MMM-0.05P) and (e-f) MWCNTs-F (MMM-0.05F).

3.1.2 Membrane Performance towards CO_2 . The gas separation performance for membranes was first evaluated by conducting a single gas permeation test followed by a kinetic sorption study. From this single gas permeation test, the permeance of the membranes towards CO_2 could be ascertain, enabling optimized MWCNTs loading for greater membrane separation. Gas permeation properties of MMMs incorporated with pristine and functionalized CNTs were initially investigated and compared to the neat CA membrane. It was observed that the CO_2 permeance of the MMM-0.05P (270.242 ± 0.069 GPU) and MMM-0.05F (374.513 ± 0.102 GPU) were higher than the pure CA membrane (131.580 ± 0 GPU), as presented in Figure 2.

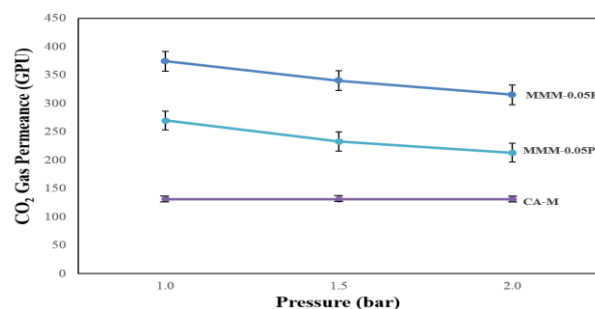


Figure 2. CO_2 Permeance for CA-M, MMM-0.05P, and MMM-0.05F

Based on Figure 2, a higher CO₂ permeance was obtained when MWCNTs-P were integrated into the CA membrane results from more free volume space available in the polymer matrix [15]. The disruption in the polymer chain packing due to the interaction between polymer segmental chains and CNTs ultimately leads to more void spaces in the membrane formed [16]. Thus, an increase in the overall permeance is a direct consequence of these reasons.

Meanwhile, when MWCNTs-F are embedded into CA polymer matrix, the CO₂ permeance continues to increase due to the functionalizing of CNTs [10, 12]. Functionalization shortens and opens up the ends of the MWCNTs, creating an open ended structure covered with a uniform coating of β -CD. Fast transport of gases are possible by the forming of these smooth nanochannels CNTs walls [17]. This inadvertently causes favourable CO₂ permeance improvements [15]. Apart from this, the functionalized CNTs have better CO₂ permeance due to the availability of the hydroxyl functional group on the β -CD. This helps improve the solubility of CO₂ in the MMM from the strong interaction present between the CO₂ molecules and the functional groups on the MWCNTs-F [18].

3.1.3 Transient Sorption and Diffusivity of the Membrane. Subsequently, the membrane performance was also determined through the Kinetic Sorption Study. This was because the gas transport through dense membrane are normally governed through the solution-diffusion mechanism [19]. Effectively, this emphasizes the solubility of specific gasses and its diffusion through the membrane. Hence, gas separations are dependent not only on the diffusion capabilities of the gasses but also on the physical and chemical interactions between the gas species and the polymers affecting the quantity of gas that can be accumulated within the polymer matrix. For a deeper and clearer understanding on the transport phenomena of CO₂ through the MMMs, the kinetic coefficients were calculated and ascertained [12].

Based on Figure 3, the time spent to reach its equilibrium adsorption was in the order of CA-M > MMM-0.05F > MMM-0.05P. The reason behind this difference was the increment in the membrane's capability to adsorb more CO₂, as calculated from the TGA results (0.46365 mg for CA-M, 0.05883 mg for MMM-0.05P, and 0.074 mg for MMM-0.05F). Hence, a greater adsorption capacity would definitely incur a longer equilibrium time as compared to a smaller one.

Another aspect compared through the sorption study was the solubility coefficient of the CO₂ gas through the neat CA membrane, MMM-0.05P and MMM-0.05F. Referring to Figure 4, MMM-0.05P has the lowest CO₂ solubility coefficient among all the membranes. This was caused mainly by the agglomeration of CNTs in the polymer matrix due to the strong van der Waals forces among the pristine CNTs [13]. The embedment of MWCNTs-P into the CA polymer affects long-term stability of the dope along with the membrane's phase separation kinetics becoming one of the causes of agglomeration to be found in the membrane. Dope stability is concerned about the MWCNTs particles capability of homogeneously dispersing in a solution. Factors that influence the stability include the affinity of the MWCNTs with other constituents of dope and rate of particle settling [20]. At the same time, the solubility coefficient of CO₂ has been improved by more than a factor of 2.6, from $0.9399 \times 10^{13} \text{ cm}^3 \text{ (STP)/cm}^4 \cdot \text{cm Hg}$ (CA-M) to $2.4968 \times 10^{13} \text{ cm}^3 \text{ (STP)/cm}^4 \cdot \text{cm Hg}$ (MMM-0.05F) when functionalized MWCNTs were embedded within the CA polymer matrix. This was due to the dispersed CNTs within the polymer matrix when β -CD was used to functionalize the MWCNTs that might help to improve the CO₂ solubility of the gas molecules through strong interactions and prevents agglomeration [18]. On the other hand, the implementation of the kinetic sorption study enabled a comparative analysis of the incorporation of MWCNTs on the membrane's CO₂ diffusion coefficient ($1.4 \times 10^{-11} \text{ cm}^2/\text{s}$ for CA-M, $3.0 \times 10^{-11} \text{ cm}^2/\text{s}$ for MMM 0.05P, and $1.5 \times 10^{-11} \text{ cm}^2/\text{s}$ for MMM 0.05F). Referring to these results, numerically there are significant changes in the membranes ability to diffuse CO₂. This would infer that the embedding of CNTs does affect the CO₂ diffusion coefficient especially for MMM-0.05P.

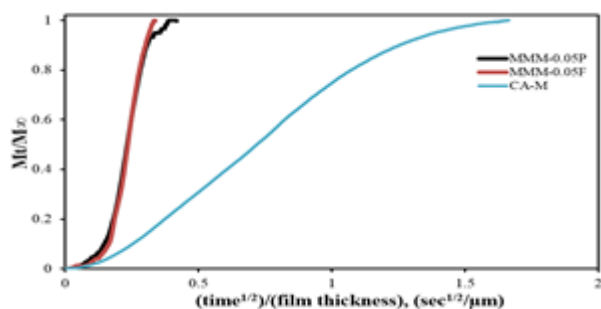


Figure 3. CO₂ Uptake Curves for CA-M, MMM-0.05P, and MMM-0.05F

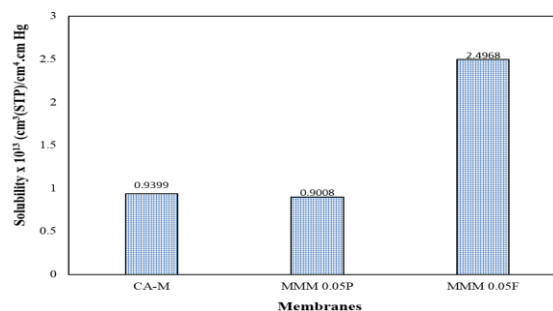


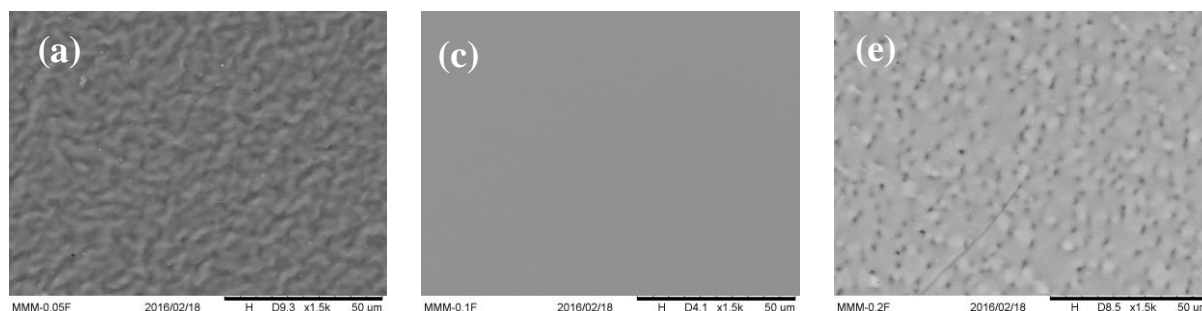
Figure 4. CO₂ solubility coefficient of CA-M, MMM-0.05P, and MMM-0.05F

3.2 Effect of Concentration Loadings of Functionalized MWCNTs

3.2.1 Membrane Characterization. As mentioned earlier, SEM characterization would enable correlative MWCNTs loading effects towards membrane structure and evaluating the successfulness of the polymer-CNTs integration. Figures 5 displays the surface and cross section micrographs of MMM-0.05F, MMM-0.1F and MMM-0.2F. Structurally, the MMM-0.1F displays a smooth and defect free membrane structure with a dense skin layer responsible for enhanced gas selectivity capabilities as compared to MMM-0.05F and MMM-0.2F. Meanwhile, MMM-0.05F and MMM-0.2F were shown to possess a compact and a porous structure surface in Figures 5a,b,e and f.

Furthermore, MMM-0.1F also displays a very compact and thin matrix near the membrane/air interface supported by a finger structure. MWCNTs-F macromolecular densification which overcomes the development of surface defects and agglomerated structures is the reason behind all the aforementioned better membrane structural buildup [21]. Vertical directed membrane/air interface densification led to the formation of a thin dense-skin layer suppressing the pin hole surface defects. Lastly, a better polymer-particle interaction and compatibility was induced from the strong adhesion between the CA polymer and MWCNTs-F. All of this contributes in forming a defect free skin layer [21]. However at high loadings of 0.2 wt%, there is an increased chance of agglomeration. This was tentatively observed through Figure 5b-c and schematically described by Ahmad et al. [10].

The casting dope solution viscosities for different functionalized MWCNTs loadings were calculated ($282.183 \pm 0.65\text{cP}$ for CA-M, $512.750 \pm 7.00\text{cP}$ for MMM-0.05F, $554.475 \pm 5.02\text{cP}$ for MMM-0.1F, and $992.333 \pm 1.44\text{cP}$ for MMM-0.2F). Based on these results, the viscosity of the casting solution increased with increased the MWCNTs loading which is in line with the SEM images (Figure 5). At such a high viscosity of $992.333 \pm 1.44\text{cP}$ was at 0.2 wt% CNTs. Where, the membrane morphology would have a highly dense and compact packing layer (Figure 5f). This was due to the diffusion of the phase inversion was suppressed as the rheological hindrance from the agglomeration of CNTs causing delayed exchange between the solvent and non-solvent [22].



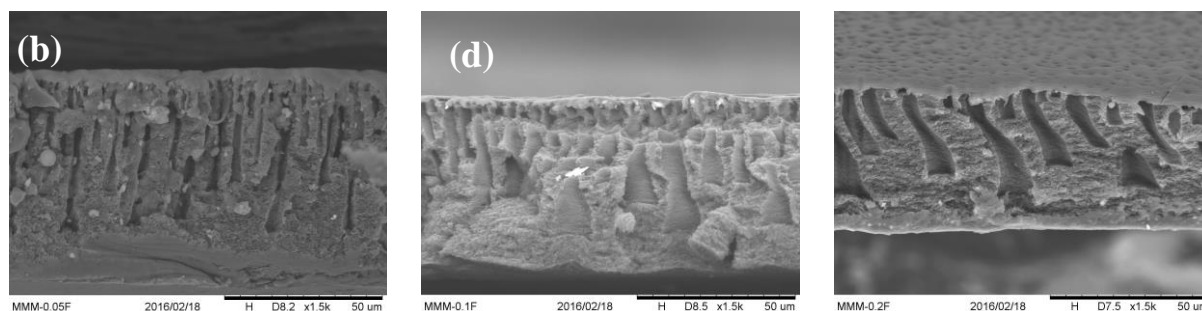


Figure 5. SEM morphologies of surface and cross section of mixed matrix membrane at different MWCNTs-F loadings of (a-b) 0.05 wt%, (c-d) 0.1 wt%, and (e-f) 0.2 wt%.

3.2.2 Membrane Performance towards CO₂. The MMMs with 0.05 wt%, 0.1 wt% and 0.2 wt% MWCNTs-F underwent the single gas permeation test to find the relationship between CNTs loadings and the CO₂ permeance. Figure 6 showed that MMM-0.1F possesses the greatest CO₂ permeance of $1017.288 + 0.613$ GPU as compared to MMM-0.05F ($374.513 + 0.102$ GPU) and MMM-0.2F ($117.184 + 0.068$ GPU). This remarkable difference could be attributed to the good interfacial interaction between MWCNTs and polymer matrix [23]. In addition, it might be due to increase the availability of fast smooth nanochannels for gas transport along with better solubility from more β -CD in the membrane [18].

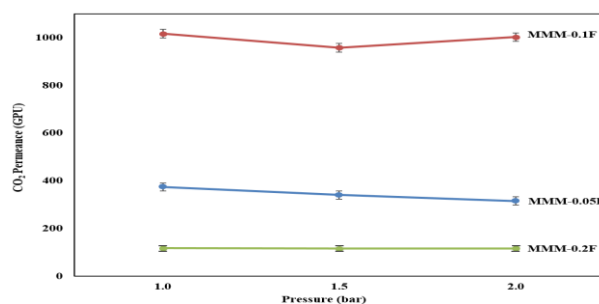


Figure 6. CO₂ Permeance for MMM-0.05F, MMM-0.1F, and MMM-0.2F.

3.2.3 Transient Sorption and Diffusivity of the Membrane. Likewise, the effect of the CNTs loading on the membrane performance was also evaluated through the Kinetic Sorption Study. Based on Figure 7, it can be seen that MMM-0.1F and MMM-0.2F reaches its CO₂ adsorption equilibrium slower than MMM-0.05F. This was due to the increment in the membrane's capability to adsorb CO₂ quantified from the difference in weight measured by the TGA (0.074 mg for MMM-0.05F, 0.78521 mg for MMM-0.1F, and 0.71894 mg for MMM-0.2F). A higher adsorption potential would naturally prolong the membranes from achieving its maximum adsorption state.

Based on Figure 8, the MMM-0.1F had the highest CO₂ solubility coefficient of 14.9601×10^{13} cm³ (STP)/cm⁴.cm Hg as compared to MMM-0.05F (2.4968×10^{13}) cm³ (STP)/cm⁴.cm Hg and MMM-0.2F (1.4648×10^{13}) cm³ (STP)/cm⁴.cm Hg. This was due to the well dispersed inorganic filler and the controlled amount of functionalized MWCNTs within the CA polymer matrix which further improve the MMM separation performance [21, 24, 25].

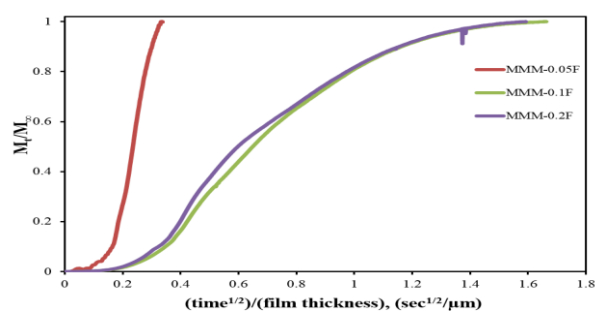


Figure 7. CO₂ Uptake Curves of CO₂ Permeance for MMM-0.05F, MMM-0.1F, and MMM-0.2F

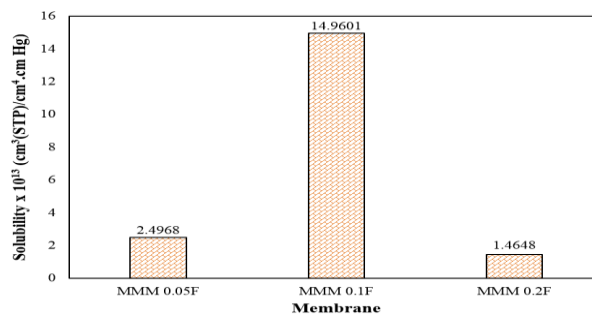


Figure 8. CO₂ solubility coefficient of CO₂ Permeance for MMM-0.05F, MMM-0.1F, and MMM-0.2F.

In this study, the CO₂ diffusion coefficients membrane diffusivity were also determined (1.5×10^{-11} cm²/s for MMM 0.05F, 6.8×10^{-12} cm²/s for MMM 0.1F, and 8.0×10^{-12} cm²/s for MMM 0.2F). Based on these results, it can be observed that CO₂ diffusion coefficient was the highest when 0.05% of MWCNTs was embedded into the CA polymer matrix. Meanwhile, it reduced when the MWCNTs concentration was increased to 0.1 wt%. These results have proved that the CO₂ diffusion coefficient was mainly affected by the membrane's solubility.

In fact, diffusivity does not contribute much for improving CO₂ permeance. Conversely, in this study the solubility can be effectively increased the CO₂ permeance. In short, these results proved that the driving force in the transport of CO₂ is to be controlled by the solubility and in direct agreement with a closely related kinetic adsorption study [12].

Lastly, this present work was compared to another research work Jawad et al. [12] as depicted in Table 2. Based on Table 2, the low acetyl content of 39% improved the CO₂ permeance to 1017.29 GPU and solubility coefficient to 14.960×10^{13} cm³ (STP)/cm⁴.cmHg. This is in agreement with Puleo et al (1989) which conclude that a lower acetyl group content would reduce the plasticization along with permeance and solubility coefficients [26].

Table 2. Summary of the permeation properties achieved by the present work compared to other research works.

References	Polymer	Filler	P _{CO2} (GPU)	CO ₂ solubility coefficient (cm ³ (STP)/cm ⁴ .cmHg)	CO ₂ diffusion coefficient (cm ² /s)	Acetyl Content
Present work	CA	MWCNTs-F 0.10 wt%	1017.29	14.960×10^{13}	6.8×10^{-12}	39%
Jawad et al. [12]	CA	MWCNTs-F 0.10 wt%	741.67	198.352×10^{11}	3.70×10^{-11}	54.6-56%

4. Conclusion

In summary, the optimal MWCNTs-F loading was ascertained to be 0.1 wt% as it has the highest CO₂ permeance of 1017.288 ± 0.613 GPU and CO₂ solubility coefficient through the membrane along with a smooth and defect morphology. Solubility was improved as the loading increased reaching its highest values of 14.9601×10^{13} cm³ (STP)/cm⁴.cm Hg due to the presence of more β -CD in the MMMs. However, at higher loadings the solubility reduced due to the agglomeration of CNTs in the polymer matrix. Kinetic adsorption studies also uncovered that the main transport of CO₂ gasses in MMMs are determined by its solubility. Hence, greater emphasis in enhancing membrane solubility coefficient towards CO₂ can significantly create superior gas separation performance and apply the solution-diffusion mechanism.

Acknowledgements

The authors would like to offer their appreciation to the Ministry of Higher Education Malaysia (MOHE) for approving Fundamental Research Grant Scheme (FRGS) (MOHE Ref No: FRGS/1/2015/TK02/CURTIN/03/01) and Cost Centre: 001048. We would also like to thank LRGS USM (Account No: 304/PJKIMIA/6050296/U124) and Curtin Cost Centre: 001047.

References

- [1] Haszeldine R S 2009 *Science* **325** 1647
- [2] Speight J G 2007 *Natural Gas: A Basic Handbook*. Elsevier Science
- [3] Leung D Y C, Caramanna G and Maroto-Valer M M 2014 *Renew. Sust. Energ. Rev.* **39** 426
- [4] Baker R W 2002 *Ind. Eng. Chem. Res.* **41** 1393
- [5] Han S H and Lee Y M 2011 Recent High Performance Polymer Membranes for CO₂ Separation. In *Membrane Engineering for the Treatment of Gases: Gas-Separation Problems with Membranes* (vol 1) The Royal Society of Chemistry Chapter 4 pp 84-124
- [6] Drioli E, Barbieri G and Pullumbi P 2011 *Membrane Engineering for the Treatment of Gases*. Royal Society of Chemistry
- [7] Cong H, Radosz M, Towler B F and Shen Y. 2007 *Sep. Sci. Technol.* **55** 281
- [8] Skoulidas A I, Ackerman D M, Johnson J K and Sholl D S 2002 *Phys. Rev. Lett.* **89** 185901
- [9] Mahajan R and Koros W J 2000 *Ind. Eng. Chem. Res.* **39** 2692
- [10] Ahmad A L, Jawad Z A, Low S C and Zein S H S 2014 *J. Membr. Sci.* **451** 55
- [11] Chen J, Dyer M J and Yu M F 2001 *J. Am. Chem. Soc.* **123** 6201
- [12] Jawad Z A, Ahmad A L, Low S C, Chew T L and Zein S H S *J. Membr. Sci.* **476** 590
- [13] Sahoo N G, Rana S, Cho J W, Li L and Chan S H 2010 *Prog. Polym. Sci.* **35** 837
- [14] Ma P C, Kim J K and Tang B Z 2007 *Composites Science and Technology* **67** 2965
- [15] Sanip S M, Ismail A F, Goh P S, Soga T, Tanemura M and Yasuhiko H 2011 *Sep. Purif. Technol.* **78** 208
- [16] Cong H, Zhang J, Radosz M and Shen Y 2007 *J. Membr. Sci.* **294** 178
- [17] Sanip S M, Ismail A F, Goh P S, Ng B C, Abdullah M S, Soga T, Tanemura M and Yasuhiko H. 2010 *Nano.* **05** 195
- [18] Kim S, Jinschek J R, Chen H, Sholl D S and Marand E 2007 *Nano Letters* **7** 2806
- [19] Paul D R and Yampol'skii Y P 1993 *Polymeric Gas Separation Membranes* Taylor & Francis
- [20] Ismail A F, Rahim N H, Mustafa A, Matsuura T, Ng B C, Abdullah S and Hashemifard S A 2011 *Sep. Purif. Technol.* **80** 20
- [21] Aroon M A, Ismail A F, Montazer-Rahmati M M and Matsuura T 2010 *J. Membr. Sci.* **364** 309
- [22] Choi J H, Jegal J, Kim W N 2006 *J. Membr. Sci.* **284** 406
- [23] Khan M M, Filiz V, Bengtson G, Shishatskiy S, Rahman M M, Lillepaerg J and Abetz V 2013 *J. Membr. Sci.* **436** 109
- [24] Khan M M, Filiz V, Bengtson G, Shishatskiy S, Rahman M and Abetz V 2012 *Nanoscale Res. Lett.* **7** 504
- [25] Kim S, Chen L, Johnson J K and Marand E 2007 *J. Membr. Sci.* **294** 147
- [26] Puleo A, Paul D and Kelley S 1989 *J. Membr. Sci.* **47** 301